result, both the LP- and the IP-compressor stage groups revealed high-frequency, short-duration mass flow fluctuations with large amplitudes and alternatively positive and negative values. The HP-compressor stage group exhibited only positive mass flow fluctuations. These fluctuations were apparently propagated downstream and did not originate from the HP part. Introducing the stator blade stagger angle adjustment brought substantial change in operational behavior. Adjusting the LP- and IP-compressor stagger angle caused a significant shift in surge limit and established a fully stable operation regime for all three compressor parts.

References

[1]Schlichting, H., "Die Grenzschicht mit Absaugung und Ausblasen," Luftfahrtforschung, No. 19, 1942, pp. 239–301.

[2]Betz, A., "History of Boundary Layer Control in Germany," *Boundary Layer and Flow Control*, Vol. 1, 1961, pp. 1–20.

[3]Greitzer, E. M., "Stability of Pumping Systems," *Journal of Fluids Engineering*, Vol. 103, June 1981, pp. 193–238.

[4]Schobeiri, M. T., "New Shock Loss Model for Transonic and Supersonic Axial Compressors with Curved Blades," *Journal of Propulsion and Power*, Vol. 14, No. 4, 1998, pp. 470–478.

[5]Schobeiri, M. T., "Active Aerodynamic Control of Multi-stage Axial Compressor Instability and Surge by Dynamically Adjusting the Stator Blades," American Society of Mechanical Engineers, ASME-Paper GT-0479, June 2001.

[6]Attia, M. S., and Schobeiri, M. T., "A New Method for the Prediction of Compressor Performance Maps Using One-Dimensional Row-by-Row Analysis," American Society of Mechanical Engineers, ASME-Paper 95-GT-434, June 1995.

[7]Schobeiri, M. T., Abouelkheir, M., and Lippke, C., "GETRAN: A Generic, Modularly Structured Computer Code for Simulation of Dynamic Behavior of Aero- and Power Generation Gas Turbine Engines," *Journal of Gas Turbine and Power*, Vol. 1, July 1994, pp. 483–494.

Aerodynamic Design of a Vertical-Thrust Adapter for Jet Engines

T. Strand*
San Diego, California 92107

Introduction

SUPPOSE we want to change the direction of the thrust of the jet engines of a hypothetical stationary multiengined vertical takeoff and landing (VTOL) aircraft from horizontal to vertical. One approach might be to tilt each engine 90 deg. Another might be to tilt the exhaust nozzles only. A third and possibly simpler approach might be, if feasible, to guide the horizontal flow, issuing from each nozzle, through a right angle turn by having it follow along a two-dimensional curved barrier. This latter, novel concept is the subject of the present aerodynamic design study.

To obtain two-dimensional flow, we shall assume that the cross section of the exhaust nozzle, instead of being circular, is square, and that the jet is constrained to flow along a curved barrier between two vertical walls (endplates) attached to the sides of the barrier. The flow model assumed and the coordinate system used are shown in Fig. 1a.

The barrier blocks the horizontal flow and turns the flow downward through a right angle. We shall assume the barrier to consist of a curved constant-velocity (streamline) section, conjoined to two straight sections, one of which is attached to the nozzle. The straight sections serve to guide the decelerating flow to—and the accelerating flow from—the curved section. Two free streamlines, extending to infinity downstream, complete the description of the thrust adapter.

Hence, we shall be dealing with a two-dimensional gas flow in which the bounding walls are either straight or have constant velocity. Textbooks on compressible fluid flow (see for instance Refs. 1–4) show that the solution to this type of configuration can be obtained by modifying the solution to its incompressible flow counterpart, provided the Chaplygin–Karman–Tsien tangent-gas approximation is substituted for the isentropic relations. In the counterpart (related) flow the lengths of—and the velocity magnitudes along—the boundaries are different from those in the compressible flow, but the velocity inclination angles are identical at corresponding points. We shall, therefore, first obtain the solution to the incompressible flow problem. Next, this solution will be modified for compressibility.

No new theories or methods will be introduced. Textbook aerodynamic theory will be employed to calculate the shape of a sample unique barrier and the pressure coefficients along the boundaries.

Several authors have studied other two-dimensional configurations having boundaries consisting of combinations of straight lines and free streamlines. Some of these are discussed in Ref. 4.

Incompressible Flow Solution

The problem will be formulated as a boundary-value problem and will be solved through use of a conformal mapping scheme. Consider then the incompressible flow within the boundaries ABB′CDEA′ in Fig. 1a. One flow property must be specified along each boundary.

The pressure is constant along the two free streamlines AB and EA′. The velocity magnitude q therefore has some constant value here, say U_0. Across the nozzle exhaust BB′ and along the straight section B′C, the inclination angle θ of the velocity vector is zero. Along the curved section C D, the velocity magnitude will be assumed constant, say U_1. The angle of the straight section DE will also be assumed given, say θ_1. Note that this angle is negative in the chosen coordinate system. We shall also specify a point value U_2 of the velocity magnitude at B′. Thus, after nondimensionalizing the given velocity magnitudes, we end up with three input parameters for the related incompressible flow, namely, U_1/U_0, U_2/U_0, and θ_1.

As just mentioned, the jet issues normal to the nozzle exhaust plane. Therefore, the velocity potential φ is constant along this

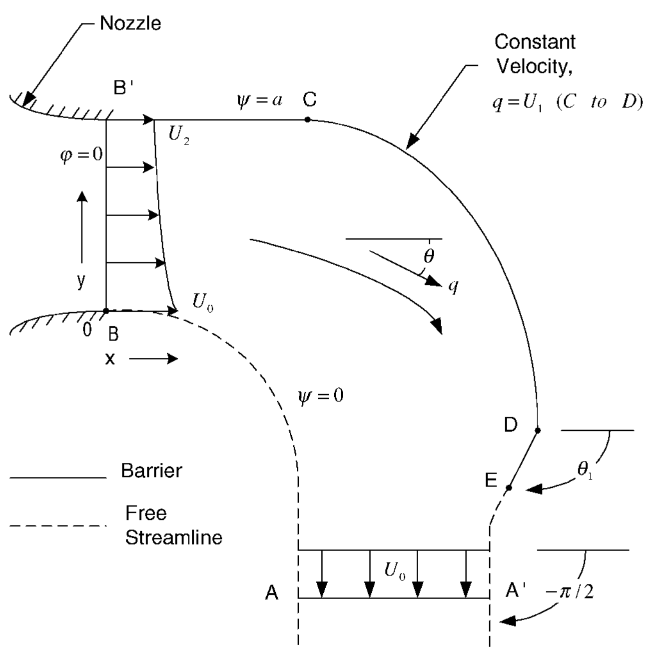

Fig. 1 Adapter, side view—flow model and coordinate system; and shape (to scale) of barrier and free streamlines for $M_0 = 0.95$, $U_1^*/U_0^* = 0.25$, $U_2^*/U_0^* = 0.92$, and $\theta_1 = -105$ deg.

Received 19 November 2001; revision received 30 October 2002; accepted for publication 8 November 2002.

*Former Member AIAA, Aeronautical Engineer, retired.

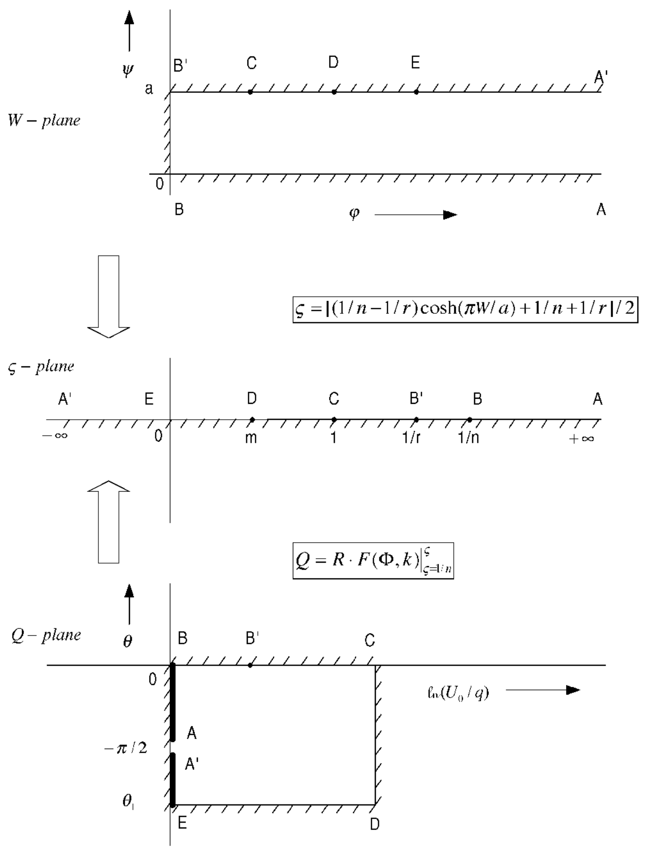

Fig. 2 Conformal mapping planes.

boundary. Because a potential is only determined up to an arbitrary constant, we might as well select φ to be zero along BB′.

The stream function ψ has arbitrarily been assigned the value zero along the free streamline AB and the constant value a along the boundary B′CDEA′. Let us now define t_0 to be the (so far unknown) asymptotic width of the jet. Then the volume flow $a = U_0 t_0$.

With the boundary conditions thus clearly defined, we can proceed with a simple conformal mapping scheme involving three planes (Fig. 2). First, the complex potential W plane ($W = \varphi + i\psi$) is mapped onto the upper half-plane of an auxiliary ς plane through the Schwarz–Christoffel transformation shown in the figure. Expressions for calculating the mapping constants r and n will be obtained later. Next, the hodograph plane, defined by $Q = \ln(U_0/q) + i\theta$, is mapped on to the same upper half plane. Here (q, θ) is the velocity vector in polar coordinates at any point in the flowfield. This is accomplished by mapping the four corners of the rectangle in Fig. 2 on to the four points 0, m, 1, and $1/n$ on the real axis of the ς plane by the Schwarz–Christoffel transformation shown, which was obtained from the integration tables of Ref. 5. Here, $F(\Phi, k)$ is the incomplete elliptic integral of the first kind with amplitude Φ and modulus k, where $0 \leq k \leq 1$. Consideration of the boundary points C and D in the ς plane yielded the integration constant

$$R = \ln(U_1/U_0)/K(k') = \theta_1/K(k) \tag{1}$$

where $K(k)$ is the complete elliptic integral of the first kind with modulus k ($k'^2 = 1 - k^2$). The value of k is now determined because both U_1/U_0 and θ_1 are given parameters. Reference 5 shows that

$$(1 - m)/(1 - mn) = k^2 \tag{2}$$

Also according to Ref. 5, the velocity magnitudes and inclination angles along the four boundaries can be expressed as follows (the two free streamlines are considered a single boundary):

1) Across BB′ and along B′C:

$$q/U_0 = \exp\{[1 - F(\Phi, k')/K(k')]\ln(U_1/U_0)\} \tag{3}$$

where

$$\Phi = \sin^{-1}\sqrt{\frac{1 - mn}{1 - n}\left(\frac{\zeta - 1}{\zeta - m}\right)} \quad \text{and} \quad 1/r \leq \zeta \leq 1/n \quad \text{or} \quad 1 \leq \zeta \leq 1/r$$

2) Along CD:

$$\theta = \theta_1[1 - F(\Phi, k)/K(k)] \tag{4}$$

where

$$\Phi = \sin^{-1}\sqrt{\frac{1 - m}{(1 - m)\zeta}} \quad \text{and} \quad m \leq \zeta \leq 1$$

3) Along DE:

$$q/U_0 = (U_1/U_0)^{F(\Phi, k')/K(k')} \tag{5}$$

where

$$\Phi = \sin^{-1}\sqrt{\frac{(1 - mn)\zeta}{m(1 - n\zeta)}} \quad \text{and} \quad 0 \leq \zeta \leq m$$

4) Along AB and EA′:

$$\theta = \theta_1 F(\Phi, k)/K(k) \tag{6}$$

where

$$\Phi = \sin^{-1}\sqrt{\frac{1 - n\zeta}{1 - \zeta}} \quad \text{and} \quad -\infty \leq \zeta \leq 0 \quad \text{or} \quad 1/n \leq \zeta \leq +\infty$$

Together, the expression for ζ (see Fig. 2) and Eqs. (3–6) constitute, for our purposes, the complete solution of the incompressible flow problem and yield $(q/U_0, \theta)$ as functions of $(\varphi/a, \psi/a)$. These functional relations are needed to calculate the x^* and y^* coordinates of the compressible flow, as will be shown later. The superscript $*$ will be used consistently to denote compressible flow parameters.

The mapping constants n, m, and r can be determined, respectively, from Eq. (6) when $\zeta = \infty$; from Eq. (2); and from Eq. (3) when $q = U_2$.

Compressible Flow

For completeness of presentation, the basic equations of compressible flow, as originally developed by Chaplygin and later modified by Karman and Tsien (see Refs. 1–4) are stated next. Every one of these relations was used in obtaining the numerical results reported in the next section.

$$q^*/U_0^* = (1 - \lambda)(q/U_0)\big/\left[1 - \lambda(q/U_0)^2\right] = \text{velocity magnitude} \tag{7}$$

$$\lambda = M_0^2\big/\left[1 + \sqrt{1 - M_0^2}\right]^2 = \text{Mach-number correction factor} \tag{8}$$

$$M = M_0\left(q^*/U_0^*\right)\Big/\sqrt{1 - M_0^2\left[1 - \left(q^*/U_0^*\right)^2\right]} = \text{local Mach number} \tag{9}$$

$$C_p^* = C_p\Big/\left[\sqrt{1 - M_0^2} + M_0^2 C_p\big/2\left(1 + \sqrt{1 - M_0^2}\right)\right] = \text{pressure coefficient} \tag{10}$$

$$\mathrm{d}x^* = \frac{1 - \lambda(q/U_0)^2}{q}\cos\theta\,\mathrm{d}\varphi - \frac{1 + \lambda(q/U_0)^2}{q}\sin\theta\,\mathrm{d}\psi \tag{11}$$

$$\mathrm{d}y^* = \frac{1 - \lambda(q/U_0)^2}{q}\sin\theta\,\mathrm{d}\varphi + \frac{1 + \lambda(q/U_0)^2}{q}\cos\theta\,\mathrm{d}\psi$$

$$= \text{coordinate correction formulas} \tag{12}$$

In textbooks the last two equations are always found combined as a single equation in complex variable form. These equations will now be nondimensionalized by dividing through by the asymptotic jet width $t_0(= a/U_0)$ to yield

$$\frac{dx^*}{t_0} = \frac{1-\lambda(q/U_0)^2}{q/U_0}\cos\theta\, d\left(\frac{\varphi}{a}\right) - \frac{1+\lambda(q/U_0)^2}{q/U_0}\sin\theta\, d\left(\frac{\psi}{a}\right) \tag{13}$$

$$\frac{dy^*}{t_0} = \frac{1-\lambda(q/U_0)^2}{q/U_0}\sin\theta\, d\left(\frac{\varphi}{a}\right) + \frac{1+\lambda(q/U_0)^2}{q/U_0}\cos\theta\, d\left(\frac{\psi}{a}\right) \tag{14}$$

A step-by-step integration of these equations gives the coordinates of any point on the boundaries of the flow. As mentioned in Ref. 1, any value of t_0 can be selected, because changing it only amounts to changing the scale of the coordinates of the compressible flow and therefore has no effect on the overall solution. We shall choose the value of t_0 so as to make the vertical height at the nozzle exhaust plane (i.e., y^* at B') equal to unity.

By equating the volume flow across the nozzle exhaust plane to the volume flow at infinity downstream, the asymptotic width of the jet can be obtained, again through a step-by-step integration, that is,

$$t_0^* = \int_0^1 \frac{q^*}{U_0^*}\, dy^* \tag{15}$$

This value of t_0^* is significant because it is a measure of the ratio of the vertical thrust to the original horizontal thrust. It is clear that t_0^* will always be less than or equal to unity. The thrust decrease is a result of the upstream effect of the presence of the barrier on the exhaust flow across the nozzle. The thrust decrease can, of course, be reduced by choosing the input parameter U_2^*/U_0^* to be closer to unity. This will, however, increase the overall length of the adapter.

Calculated Results

The following set of inputs was chosen more or less arbitrarily for a numerical calculation:

$$M_0 = 0.95, \qquad U_1^*/U_0^* = 0.25$$

$$U_2^*/U_0^* = 0.92, \qquad \theta_1 = -105\,\text{deg}$$

Using Eq. (7), the chosen velocity ratios were converted to $U_1/U_0 = 0.47$, $U_2/U_0 = 0.97$ for the counterpart incompressible flow. With these inputs it was found that $k = \sin 85$ deg; $n = 0.997, 4834$; $m = 0.7525$; and $r = 0.997, 4919$. Extreme accuracy was required to determine n and r. Equations (3–6) then gave q/U_0 and θ as functions of φ/a and ψ/a. Substitution into Eqs. (13) and (14) and integration determined the barrier shape and dimensions and the location of the free streamlines. The results are shown in Fig. 1, which serves a dual role as the flow model for the related incompressible flow and as the calculated shape, to scale, of the compressible flow configuration. The curved section of the barrier is seen to resemble a distorted quarter circle with a radius somewhat larger than unity. The lengths of the straight sections B′C and DE were found to be, respectively, 1.09 and 0.29, with unity being the height of the nozzle exit plane.

The two free streamlines become essentially parallel one unit length below the origin. The endplates, therefore, need not extend vertically below this value. The maximum horizontal dimension of the barrier is about two nozzle exhaust heights. Thus it can be concluded that the endplate areas can be limited to about 2 × 2, indicating a small compact adapter.

The variation of the pressure coefficients along the boundaries was obtained from Eq. (10) and is graphed in Fig. 3. The local Mach number along the curved portion of the barrier was found to be 0.61, as shown in the figure.

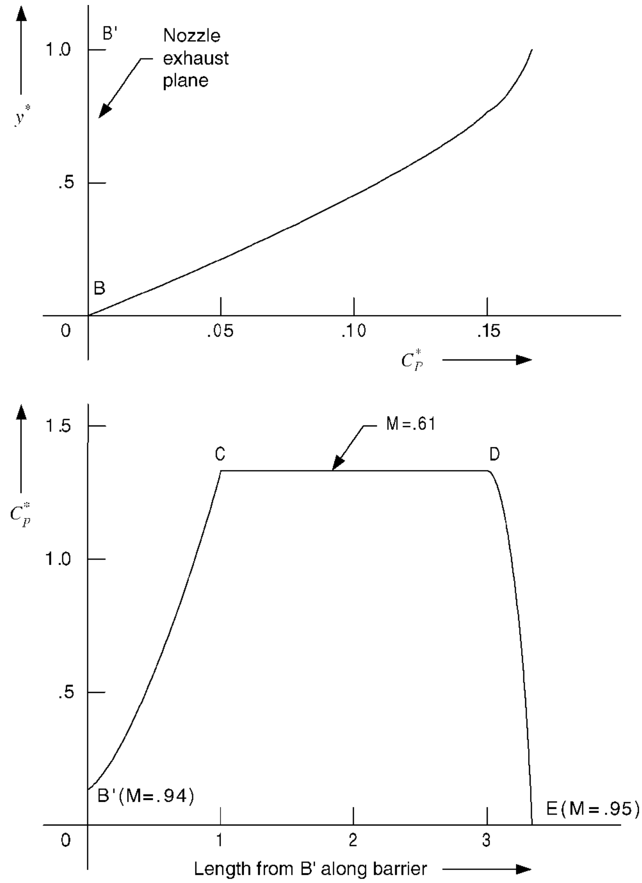

Fig. 3 Pressure distribution along barrier. $M_0 = 0.95$.

Performance of the indicated integration of Eq. (15) step by step yielded $t_0^* = 0.95$, which is in accordance with the already calculated asymptotic width of the jet (see Fig. 1). Hence, the presence of this adapter results in a 5% decrease in thrust.

Conclusions

The numerical results of the present aerodynamic design study indicate that development of a small compact adapter that alters the thrust direction of a static jet engine from horizontal to vertical might be possible.

The study is based upon an assumed flow model. The actual flow might not behave in the assumed manner. It is probable that some kind of corner guide vanes might have to be introduced to suppress flow separation and vortex formation. Experimental tests will be required for further progress.

The mathematical solution is "exact" insofar as no simplifying assumptions of any kind have been made in solving the governing fluid dynamic equations. By using the tangent-gas approximation, the results are strictly valid only for a fictitious gas, that is, a gas that is slightly different from a true isentropic gas. The error introduced increases as the local Mach number decreases from the high endpoint M_0 of tangency.

References

[1] Sedow, L. I., *Two-Dimensional Problems in Hydrodynamics and Aerodynamics*, Wiley Interscience, New York, 1965, p. 376.

[2] Shapiro, Ascher, H., *The Dynamics and Thermodynamics of Compressible Fluid Flow*, Vol. 1, Ronald, New York, 1953, p. 353.

[3] Yih, Chia-Shun, *Fluid Mechanics, A Concise Introduction to the Theory*, McGraw–Hill, New York, 1969, p. 285.

[4] Gurevich, M. I., *Theory of Jets in Ideal Fluids*, Academic Press, New York and London, 1965, p. 477, p. 489.

[5] Grobner, W., and Hofreiter, N., *Integraltafel, Unbestimmte Integrale*, Wien, Springer-Verlag, Vienna, 1961, p. 84, #8a3 (in English).